Fracture Behavior and Damage mechanisms Identification of SiC/Glass ceramic composites using DEN specimens and AE monitoring

by

V. KOSTOPOULOS[1,2*], T. LOUTAS[1] and C. DASSIOS[2]

[1]*Applied Mechanics Laboratory, Dept. of Mechanical Engineering & Aeronautics, University of Patras, Greece*

[2] *Foundation of Research and Technology Hellas, Institute of Chemical Engineering and High Temperature Processes, Stadiou str., Platani, Patras GR-26500, Greece*

[*]*Corresponding author (Tel.:+30-2610-997234, Fax: +30-2610-997237, Email: kostopoulos@mech.upatras.gr*

ABSTRACT

Large Scale Bridging in SiC/MAS-L (ceramic glass matrix) composites was investigated by using DEN specimens under tensile loading conditions with in situ Acoustic Emission monitoring. The AE data were successfully classified using Unsupervised Pattern Recognition Algorithms and the resulted clusters were correlated to the dominant damage mechanisms of the material. The evolution in time of the different damage mechanisms is feasible after the pattern recognition classification. Microscopic examination was utilised to correlate the clusters to the damage mechanism they correspond and thus to provide the failure mode identification based on AE data.

Keywords: Large Scale Bridging, Pull-out, Acoustic Emission, Unsupervised Pattern Recognition Technique

1. INTRODUCTION

It is now well established that, continuous fibre reinforcements provide a ceramic composites with the most increased fracture toughness and damage resistance. The enhanced damage resistance and increased fracture toughness of continuous fibre reinforced ceramic matrix composites (CFCCs) is due to their inherent ability to effectively redistribute stresses around holes, notches and cracks, a phenomenon which stems from the development of shielding forces in the process zone around the crack tip. Fracture in the vast majority of CFCCs is associated with the formation and propagation of macrocracks (Class I and Class II fracture) [Evans et al. 1994]. The corresponding process zone consists of two parts: the so called bridging zone with fiber bridging and pull-out developing within the macrocrack and a matrix cracking process zone ahead the macrocrack. The increase in

fracture resistance is a result of several energy-dissipating mechanisms acting in the two zones. In the matrix process zone a complex set of phenomena such as matrix microcracking, fibre/matrix interfacial debonding and transformation toughening may take place concurrently. In the bridging zone the cracked matrix is bridged by intact and/or failed fibres, which debond, slip and pull-out. The role of the bridging zone in the fracture resistance of the composite is of particular importance as the bridging fibres carry a significant portion of the applied load, hence resisting further crack opening. When the dimensions of the bridging zone are comparable to any specimen dimension, a phenomenon known as Large Scale Bridging (LSB) encountered in most CFCCs, the well established rising crack growth resistance with increasing crack extension behaviour of the composite (R-curve) is a material-extrinsic property which depends upon specimen geometry and dimensions [Cox et al. 1991,Fett et al. 2000]. To the study of the bridging effect, AE is utilised as a powerful non-destructive technique for real-time monitoring of damage development in materials and structures, which has been used successfully for the identification of the damage mechanisms in composite structures under quasi-static and dynamic-cyclic loading. The aim of the present work is to investigate the failure mechanisms in SiC/MAS-L composites by using an in-house unsupervised, Pattern Recognition (PR) technique, which proved to be capable to classify the AE data, recorded during the laboratory testing and to illuminate the different failure modes. Up to now, the majority of the proposed applications of AE for the characterization of composite materials are based on the 'Conventional' AE analysis, which usually incorporates investigation of the activity in diagrams of cumulative hits versus load and the correlation of some AE features, such as Amplitude and/or Duration, to basic damage mechanisms. Nevertheless, in the case of ceramic composites, these techniques are not sufficient due to the large number of damage and stress redistribution mechanisms, such as matrix cracking, fibre/matrix debonding and sliding, as well as stochastic fibre failure, which are active continuously during loading. In contrast, the unsupervised PR technique proposed in this work takes into consideration a large number of AE descriptors and thus, it is a more powerful tool since its multivariate approach provides detailed information for the activated damage mechanisms within the material structure and their evolution during loading.

2. EXPERIMENTAL PROCEDURE

The material used in this study is a laminated cross-ply SiC/MAS-L composite processed by EADS (ex-Aérospatiale, France). The reinforcing SiC fibres are grade Nicalon NL202 with a chemical composition in weight

concentration terms of 56.6% Si, 31.7% C and 11.7% O. The glass-ceramic matrix contains MgO, Al_2O_3, SiO_2 and LiO_2 and is made via the sol-gel route. Plates of 2.0 and 3.0 mm thickness with 8 and 12 plies respectively were produced via hot pressing. The laminae were stacked together in a symmetric $[0\text{-}90^o]_{2s}$ and $[0\text{-}90^o]_{3s}$ orientation for the 2.0 and 3.0 mm thick plate respectively. The effective volume fraction of the fibres in the loading direction is 0.17 [Brenet et al. 1996] whereas the matrix stiffness (75 GPa) and failure strain are lower than the corresponding values for the fibre and hence cracks appear first in the matrix. Typical Double Edge Notch specimens used in this study are presented schematically in Figure 1. All tensile tests were performed using a MTS Universal Testing Machine equipped with hydraulic gripping system, under displacement control, at controlled environmental conditions of 25^{o}C and 70% relative humidity. AE activity was recorded during the tensile testing of the materials. The data acquisition system used was a Mistras 2001 of Physical Acoustics Corporation. The AE signals were monitored by using two resonant transducers (NANO 30), which were attached to each specimen by means of a suitable coupling agent. Pre-amplification of 40 dB and bandbass filtering of 20-1200 kHz was performed by 2/4/6-AST pre-amplifiers.

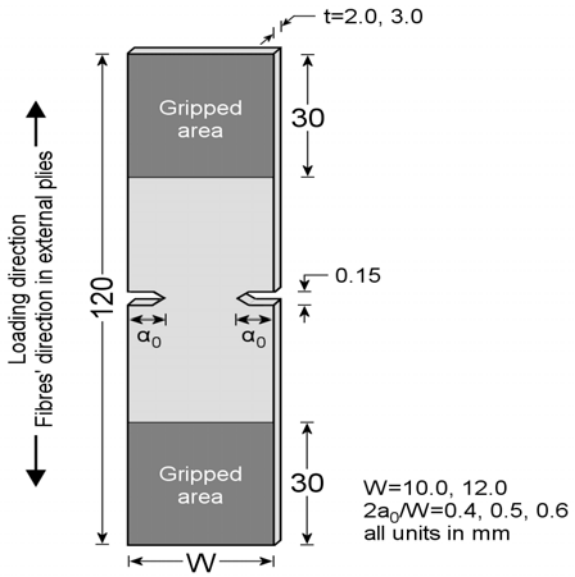

Figure 1: DEN specimens configuration

3. AE MONITORING

Acoustic emission was monitored during a number of tensile tests. The acquisition parameters for the two active channels were: threshold and gain equal to 30 and 20 dB respectively, while the Peak Definition Time (PDT), Hit Definition Time (HDT) and Hit Lockout Time (HLT), were set at 50 μs, 100 μs and 500 μs. Pencil break tests were used for the calibration of the applied set up. Figures 2,3 are two representative AE data plots. They clearly show the load drop due to the bridging effect and the significant increase of the AE activity at this point.

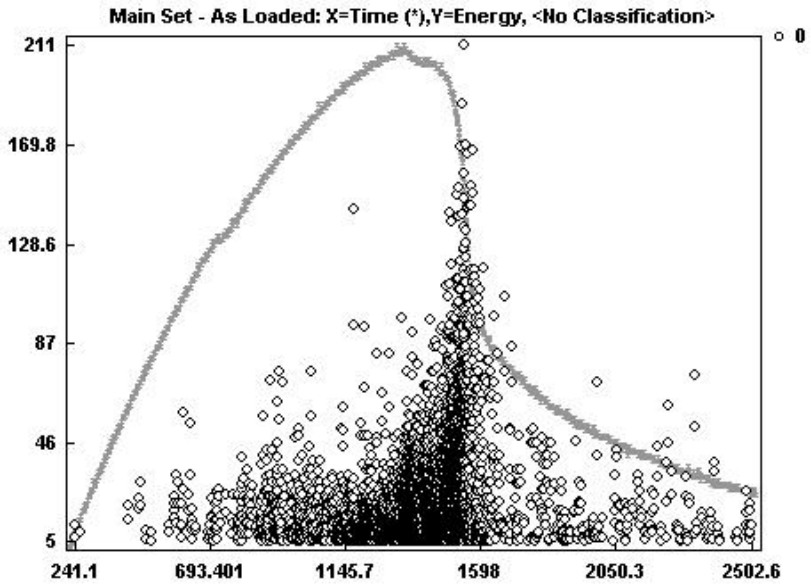

Figure 2: AE Energy vs Time

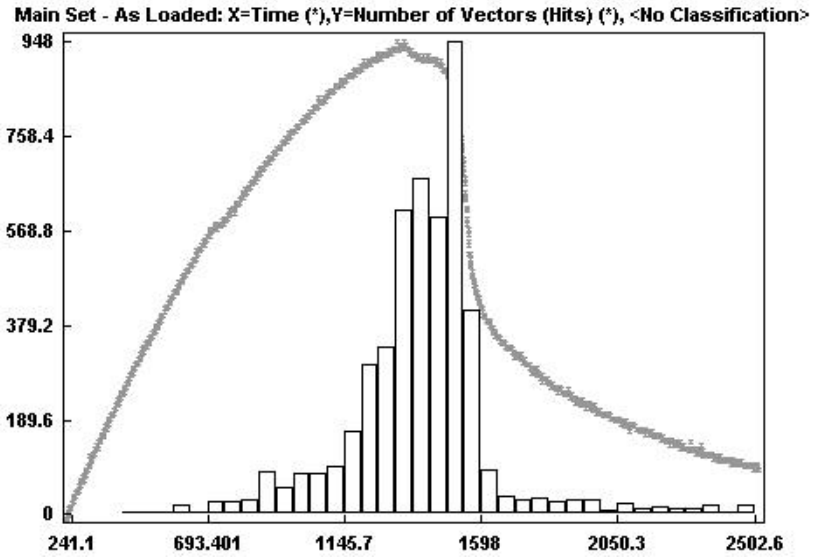

Figure 3: Distribution of AE Hits vs Time

4. PATTERN RECOGNITION

A schematic representation of the proposed pattern recognition scheme which was used for the analysis of AE signals monitored during the testing, is presented in Figure 4. Noesis Professional 3.1, software by Physical Acoustics Corporation, offered a variety of algorithms for unsupervised PR such as Maxmin Distance, Cluster Seeking, Forgy, k-means and Isodata. With the exception of Cluster Seeking (a generalized radial seeking algorithm), all the others are widely known and used in the literature [Pappas et al. 1998, Jain et a.l 1987, Anastassopoulos et al. 1995]. The determination of the initial conditions is critical for the performance of the above algorithms. A most interesting approach [Anastassopoulos et al. 1995, Loutas et al. 2002] utilizes the Maxmin Distance algorithm for a primary classification of the data and use the resulting cluster centers as initial conditions for the application of a PR algorithm.

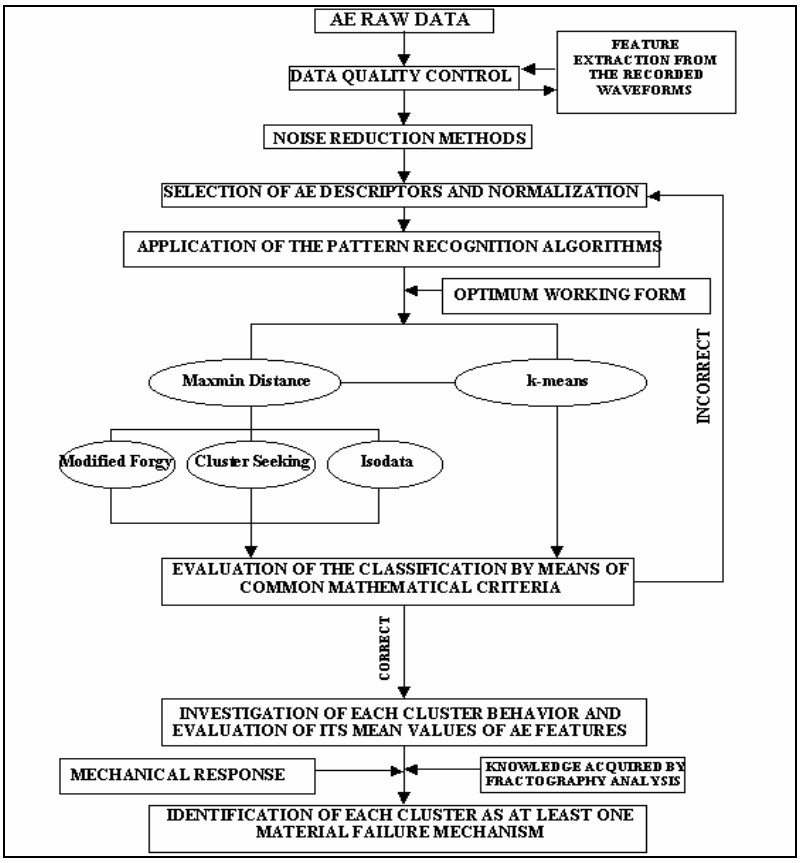

Figure 4: Pattern recognition scheme

Moreover, it was decided to test extensively all the available algorithms and check their performance for the same problem. Consequently the unsupervised PR schemes, which were used in this work, are: 1. Maxmin Distance-Forgy, 2. Maxmin Distance-Cluster Seeking, 3. Maxmin Distance-Isodata, 4. k-means. Only k-means was used alone, since it does not demand initial conditions but the number of the desired classes. A complete procedure for performing unsupervised PR was of primary importance for the authors. The main problem was the fact that every algorithm involves a number of predefined parameters which must be set by the user. These parameters determine the internal operation of the PR scheme and differ in each case. After systematic 'trial and error', a parametric analysis was conducted and the range of interest of those parameters was located as well as the step increase of their values. The clustering results are evaluated using cluster validity criteria. From a plethora of validity criteria, R criterion and τ criterion [Tou et al. 1974, Fukunaga et al. 1990] were chosen as they have the advantage of being independent with the number of classes. These two criteria give an indication of the compactness and the separation among the resulting classes. Low values for R and high values for τ reveal a successful classification and the

formation of well-defined compact clusters. The application of the above described procedure led to a 3-class clustering. The results of the pattern recognition algorithms application is shown in Figure 5 in principal axes projection.

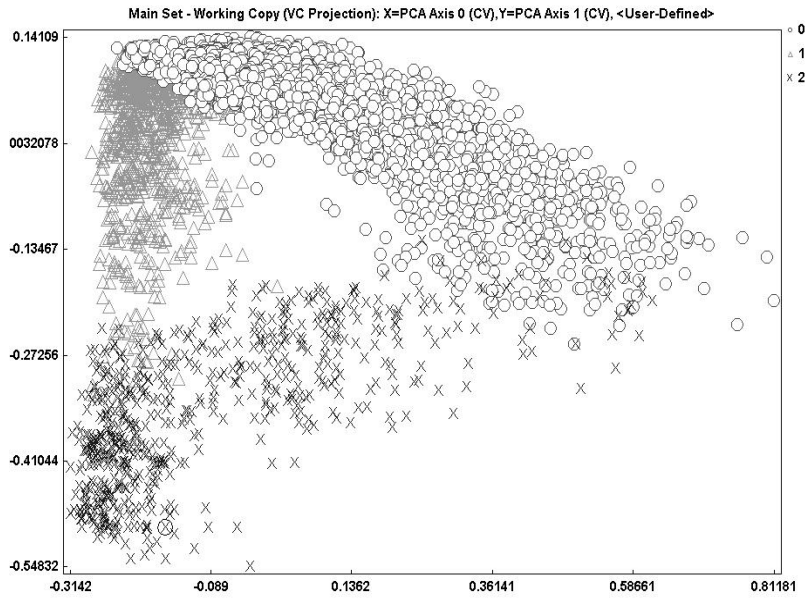

Figure 5: Principal components projection of the three resulted clusters

The classification is successful and compact clusters in the n-th dimensional space are created. In our study n equals 4 because this is the number of the chosen AE descriptors where the pattern recognition scheme is based.

5. FAILURE MODE IDENTIFICATION

After a successful, according to R and τ criteria, classification of AE data, the resulting clusters should be correlated with the material's damage mechanisms. The most demanding point of the PR approach is to identify the damage mechanisms [Barre et al. 1994, Curtis et al. 1972, Mizutani et al. 2000, Ohtsu et al. 1987 , Loutas et al. 2002] that these clusters correspond to, in order to understand the damage evaluation of the materials under investigation under quasi-static loading. This is due to the fact that the classification process does not lead to a unique solution and there do not exist any solid and indisputable criteria to determine which classification result is more appropriate and representative of the actual damage mechanisms. The first goal of a PR algorithm is to result in compact and well-

separated classes. In the present work, this is accomplished and this is proved by the values of R and τ validity indices, shown in the previous paragraph.

Towards a successful damage mechanisms identification, the mechanical behaviour of a fibre-bridged crack must be well understood. The Class I fracture characteristics (formation and development of a single macrocrack) of a brittle-matrix fibre-reinforced composite are presented in the load-displacement (F-d) behaviour of Fig. 6 together with a schematic depiction of the mechanical processes occurring during testing. During the initial loading stages, reversible mechanical phenomena occur within the composite (region O→A, stage 2 in Figure 6). The first matrix crack (point A in Figure 6) triggers the appearance of the bridging zone while cracking evolves (region A→B, stage 3 in Figure 6) until the macrocrack has fully developed, spanning the total width of the specimen (point B, stage 4 in Figure 6,). Beyond this stage, fibres start failing within the volume of the composite and the load-carrying capacity of the remaining fibres decreases until a critical number of fibres have failed (point C in Figure 6). Failed fibres undergo pull-out and an additional contribution to the recorded load arises, owing to friction at the fibre/matrix interface (region B→D, stage 5 in Figure 6). Under the global load-sharing principle, each fibre failure is followed by a uniform redistribution of the remaining load to the surviving fibres. As the portion of load that corresponds to each intact fibre is greater after the redistribution, more failures are induced and the process evolves until all fibres have failed (point D in Figure 6).

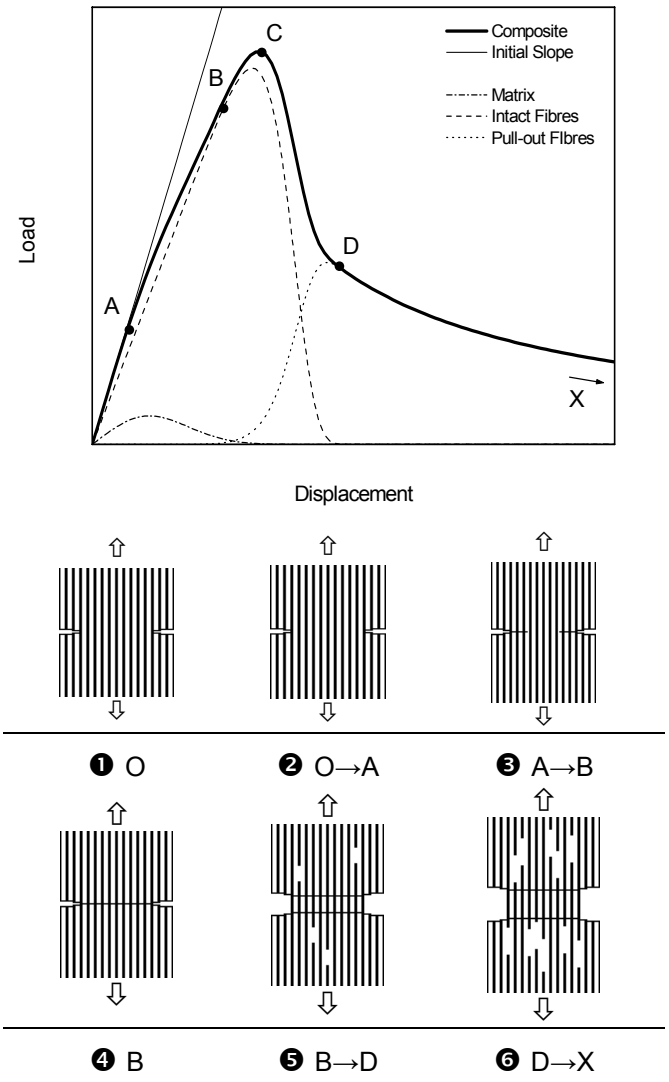

Figure 6: Load-displacement (F-d) curve typical of Class I composite fracture and schematic overview of the main fracture processes in the composite

Beyond this stage, the load carried by the composite corresponds entirely to interfacial friction due to pull-out of failed fibres (region D→X, stage 6 in Figure 6). With increasing displacement, fibre ends that were originally located at various statistical locations inside the composite are sequentially disengaged from the matrix until, eventually, the composite separates in two parts.

In summary, the main mechanisms [Dassios et al 2003] typical of Class I composite behaviour are, in order of appearance: Linear elastic composite behaviour (O→A), linear elastic fibre behaviour (A→B), crack bridging by intact and pulled-out fibres (B→D) and purely frictional bridging due pull-out of failed fibres (D→X). Accordingly,

the corresponding F-d curve of the composite is the sum of 3 individual contributions (Figure 6): A limited contribution corresponding to the load carried during the early loading stages by the fibres and the brittle matrix, a contribution corresponding to the load carried by the surviving fibres which can be assumed identical to that of a fibre bundle where load is carried by a large number of fibres acting independently and a contribution corresponding to friction by fibre pull-out. Beyond the physical understanding of the bridging phenomenon and Class I behaviour, the activation of the different clusters versus the applied load, as it is presented in Figure 7, provide an additional extremely useful piece of information.

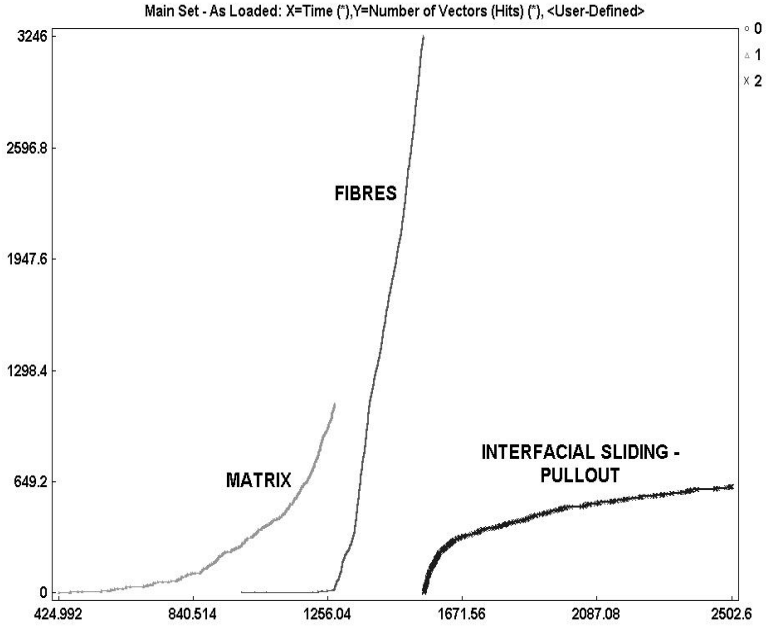

Figure 7: Cluster evolution in time

In this figure the different clusters evolution and activation is very clear. Matrix cracks dominate in the very beginning of the load rise. Since matrix cracks come to a point of saturation, stochastic fibre failure becomes the prevalent failure mechanism and is responsible for significant AE activity. In the final stage interfacial sliding due to fibre pullout is clearly shown. During monotonic tensile testing of double edge notched SiC/MAS-L specimens, the outer surface of the specimen (0^o ply) was constantly monitored through Raman microscope by using a low magnification (×4) lens focusing along the ligament between the notches. Shortly after the application of load, matrix microcracks form and develop at both notch roots at random vertical positions. The microcracks are oriented normal to the direction of loading and, with increasing load, propagate within the matrix towards the facing notch.

The phenomenon evolves until a critical crack density is established where the different paths of adjacent microcracks merge to form a dominant, fully developed macrocrack that spans the width of the ligament (fig. 8).

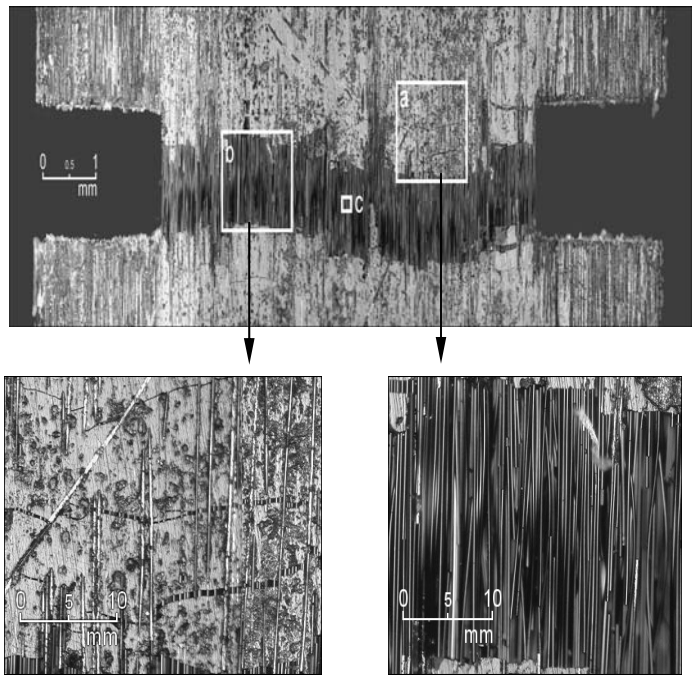

Figure 8: Large Scale Bridging in SiC/MAS-L composite: In situ microscopical damage observation during testing. Magnifications: a) Matrix microcracking during the early fracture stages, b) Fibre bridging and pull-out

Upon formation of a fully developed macrocrack, the remaining microcracks do not propagate further. In the bridging zone bridging fibres stretch, fail in the matrix and pull-out. The bridging phenomenon is particularly prominent for the material tested in this study. The pull-out contribution was also extensive owing to a weak fibre/matrix interphase.

6. CONCLUSIONS

Failure mode identification for SiC/MAS-L composites, during quasi-static tensile loading was accomplished using an unsupervised pattern recognition analysis to AE data monitored during the tests. A number of algorithms were used and the results were evaluated based on R and τ validity criteria. The cluster activation plotted against the normalized applied load, was proved very useful in the identification of the damage mechanisms of the materials.

This knowledge was supported by the assistance of extensive microscopy. Unsupervised pattern recognition proved a powerful tool for the classification of AE hits, in the case of ceramic composites, and the procedure established is repeatable and reliable.

7. ACKNOWLEDGMENTS

The authors wish to thank Mr. Patrick Peres of EADS (France) for providing the composite material used in this study.

8. REFERENCES

1. Evans, A.G. and Zok, F.W., *The physics and mechanics of fibre-reinforced brittle matrix composite,* Journal of Materials Science, V. 29, pp. 3857-3896, 1994.
2. Cox, B.N., *Extrinsic factors in the mechanics of bridged cracks,* Acta Metall. Mater., V. 37, pp.1189-1201, 1991.
3. Fett, T., Munz, D. and Geraghty, R.D., White K.W., *Influence of specimen geometry and relative crack size on the R-curve,*Eng. Fract. Mech.,V.66, pp.375-386 2000.
4. Brenet, P., Conchin, F., Fantozzi, G., Reynaud, P., Rouby, D. and Tallaron, C., *Direct measurement of th bridging constraint as a function of crack displacement in ceramic-ceramic composites,* Compos. Sci. Technol.,V.84, pp. 817-823, 1996.
5. Noesis© 3.1 Reference Manual, *Pattern Recognition & Neural Networks Software for Acoustic Emission Applications*, Ver. 3.1, *Envirocoustics ABEE*, 1999.
6. Loutas T.H., Kontsos A., Sotiriadis G., Pappas Y.Z. and Kostopoulos V., *On the identification of the damage mechanisms in oxide/oxide composites using Acoustic Emission,* Proceedings of the 25th European Conference on Acoustic Emission Testing, Prague, Czech Republic, 2002
7. Pappas Y. Z., Markopoulos Y. P. and Kostopoulos V., *Failure mechanisms analysis of 2D carbon/carbon using acoustic emission monitoring,* NDT&E International, Vol. 31(3), pp. 157-163, 1998.
8. Jain A. K., *Advances in statistical Pattern Recognition,* NATO ASI Series, V. F30, pp. 230-249, 1987.

9. Anastassopoulos A. A. and Philippidis T. P., *Clustering methodologies for the evaluation of AE from composites,* J. Acoustic Emission, Vol. 13 (1/2), pp. 11-22, 1995.

10. Fukunaga K., *Introduction to statistical pattern recognition,*2nd English edn, Academic Press, San Antonio, CA, USA, 1990.

11. Tou J. T. and Gonzales R. C., *Pattern Recognition principles,* Addison-Wesley, Reading, MA, 1974.

12. Barre S., *On the use of Acoustic Emission to investigate damage mechanisms in Glass-fibre-reinforced polypropylene,* Composite Science and Technology, V.52, pp. 369-376, 1994.

13. Curtis G. J., *The characterization of failure mechanisms by means of Acoustic Emission,* Symposium On Acoustic Emission, Imperial College, 1972.

14. Mizutani Y., Nagashima K., Takemoto M. and Ono K., *Fracture mechanism characterization of cross-ply carbon fibre composites using Acoustic Emission analysis,* NDT&E International, V. 33, pp. 101-110, 2000.

15. Ohtsu M. and Ono K., *Pattern Recognition analysis of Acoustic Emission from unidirectional carbon-fibre epoxy composites by using Autoregressive modeling,* Journal of Acoustic Emission, V.6(1), pp. 61-71, 1987.

16. K. G. Dassios, C. Galiotis, V. Kostopoulos and M. Steen, 2003 (to be published)